Efficient and labor-saving Ru/C catalysts for the transformation of levulinic acid into γ-valerolactone under mild reaction conditions

Zaira Ruiz-Bernal[a], M. Ángeles Lillo-Ródenas[a] and M. Carmen Román-Martínez[a]

[a]MCMA group, Department of Inorganic Chemistry and Materials Institute (IUMA), Faculty of Sciences, University of Alicante, Ap. 99, E-03080 Alicante, Spain. E-mail: mcroman@ua.es; Tel.: +34965903975.

Supplementary information

Tables and figures are presented in the order in which they are mentioned in the manuscript

Table S1 Parameters of the HPLC analysis.

Column Zorbax Eclipse XDB-C8 (4.6 x 150 mm, 5 µm)
Detector: DAD (wavelength: 210 and 266 nm)
Isocratic: 1 mL/min
Temperature: 25 ºC
Injection volume: 10 µL
Analysis time: 15 min

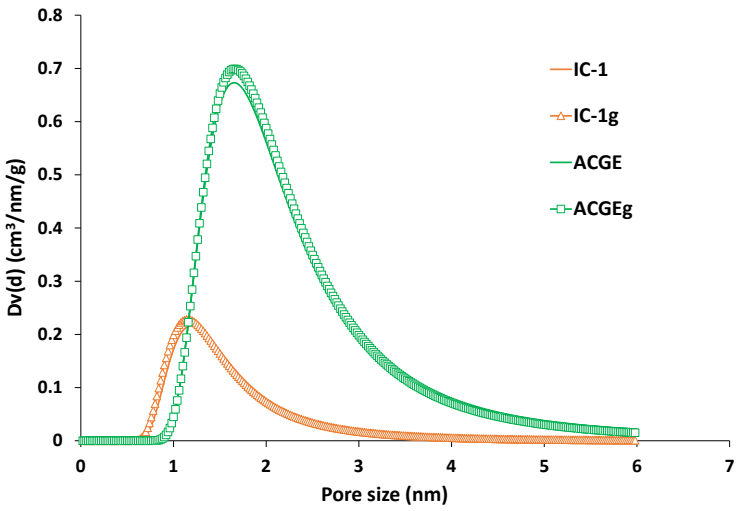

Fig. S1 Pore size distribution of carbons IC-1, IC-1g, ACGE and ACGEg. Estimated from N_2 adsorption data using the Dubinin-Astakhov equation [1].

Table S2 Textural properties of carbon supports and catalysts (as prepared and reduced).

Sample	S_{BET} [a] (m^2/g)	$V_{DR, CO2}$ [b] (cm^3/g)	$V_{DR, N2}$ [a] (cm^3/g)	$V_{meso, N2}$ [a] (cm^3/g)	$V_{meso, Hg}$ [c] (cm^3/g)	$V_{T,meso}$ (cm^3/g)	$V_{macro, Hg}$ [c] (cm^3/g)
IC-1	542	0.19	0.22	0.04	0.55	0.59	0.00
IC-1g	571	0.21	0.23	0.04	0.28	0.32	0.13
Ru/IC-1	498	0.18	0.21	0.04	0.55	0.59	0.00
Ru/IC-1g	557	0.20	0.22	0.04	0.28	0.32	0.13
Ru^R/IC-1	554	0.21	0.22	0.04	0.55	0.59	0.00
Ru^R/IC-1g	560	0.21	0.22	0.04	0.28	0.32	0.13
IC-2	2081	0.60	0.92	0.07	0.04	0.12	1.17
Ru/IC-2	1899	0.55	0.84	0.06	0.04	0.10	1.17
Ru^R/IC-2	1777	0.55	0.78	0.05	0.04	0.09	1.17
ACGE	1920	0.50	0.81	0.09	0.29	0.38	0.01
ACGEg	1991	0.52	0.85	0.09	0.22	0.31	0.05
Ru/ACGE	1876	0.50	0.80	0.08	0.29	0.37	0.01
Ru/ACGEg	1914	0.51	0.82	0.09	0.22	0.31	0.05
Ru^R/ACGE	1988	0.54	0.85	0.09	0.29	0.38	0.01
Ru^R/ACGEg	1949	0.51	0.84	0.08	0.22	0.30	0.05
SA-30	1587	0.35	0.68	0.31	0.40	0.71	0.41
Ru/SA-30	1465	0.33	0.63	0.28	0.40	0.68	0.41
Ru^R/SA-30	1505	0.31	0.64	0.30	0.40	0.70	0.41
WV-1100	1713	0.37	0.70	0.30	0.51	0.81	0.20
Ru/WV-1100	1671	0.38	0.68	0.30	0.51	0.81	0.20
Ru^R/WV-1100	1771	0.38	0.73	0.31	0.51	0.82	0.20

a: Parameters calculated from the N_2 adsorption isotherms as indicated in the text; b: Parameters calculated from the CO_2 adsorption isotherms as indicated in the text c: Parameters determined by Hg porosimetry.

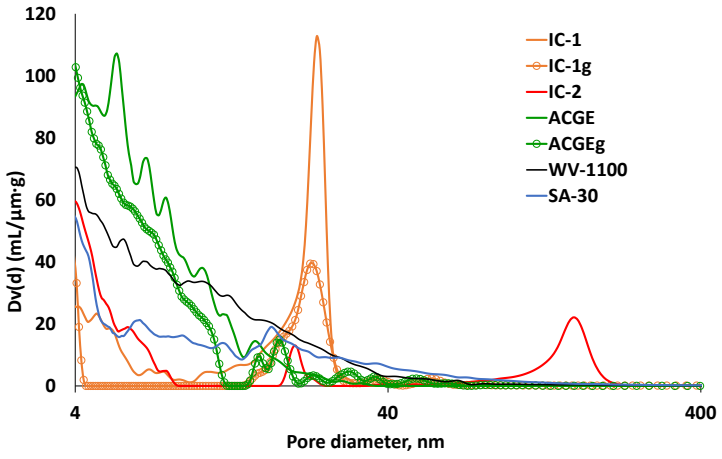

Fig. S2 Pore size distribution obtained by Hg porosimetry.

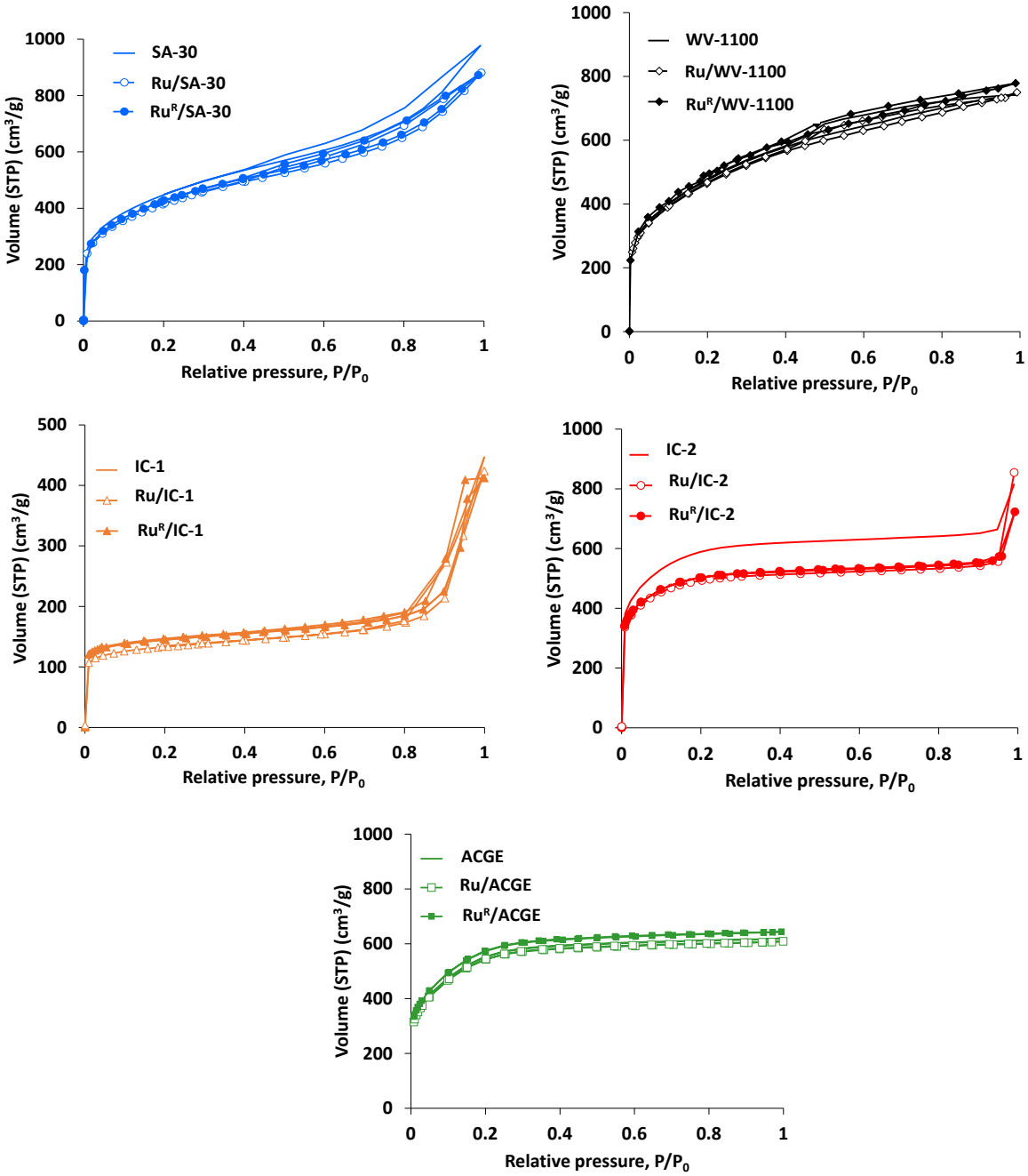

Fig. S3 N_2 adsorption-desorption isotherms at -196 °C for supports, and un-reduced and reduced catalysts.

Table S3 Average pore size of carbon materials and catalysts determined by N_2 adsorption data with the Quantachrome Quadrawin software (based in NLDFT).

Sample	Average pore size [a] (nm)
IC-1	3.7
IC-1g	4.1
Ru/IC-1	3.9
Ru/IC-1g	4.5
Ru^R/IC-1	4.2
Ru^R/IC-1g	4.3
IC-2	2.4
Ru/IC-2	3.0
Ru^R/IC-2	2.5
ACGE	2.0
ACGEg	2.0
Ru/ACGE	2.0
Ru/ACGEg	2.0
Ru^R/ACGE	2.0
Ru^R/ACGEg	2.0
SA-30	3.8
Ru/SA-30	3.7
Ru^R/SA-30	3.6
WV-1100	2.7
Ru/WV-1100	2.9
Ru^R/WV-1100	2.7

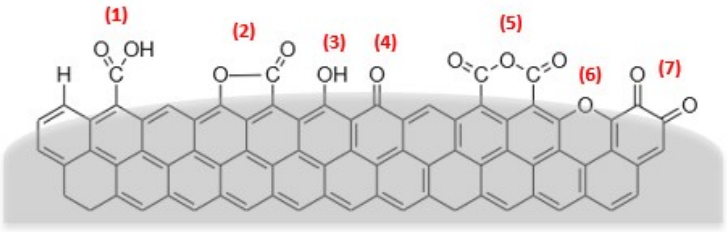

Fig. S4 Oxygen functional groups (OFG) on carbon materials.

Entry	OFG	Decomposition products	T_d (°C)
(1)	Carboxylic	CO_2	250-473
(2)	Lactone	CO_2	190-650
(3)	Phenol	CO	673-773
(4)	Carbonyl	CO	773-900
(5)	Anhydride	$CO+CO_2$	350-627
(6)	Ether	CO	773
(7)	Quinone	CO	773-980

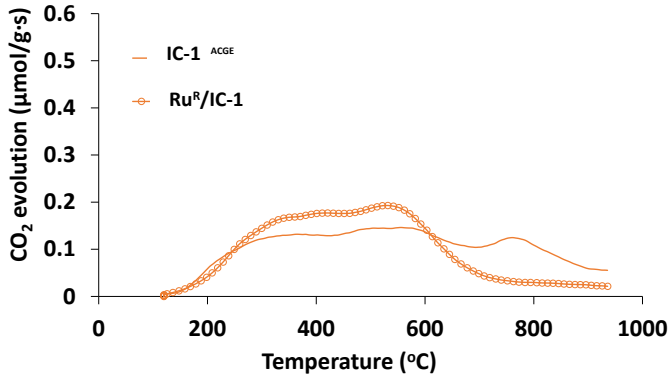

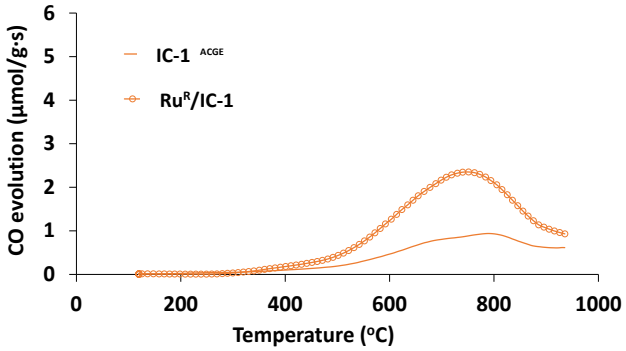

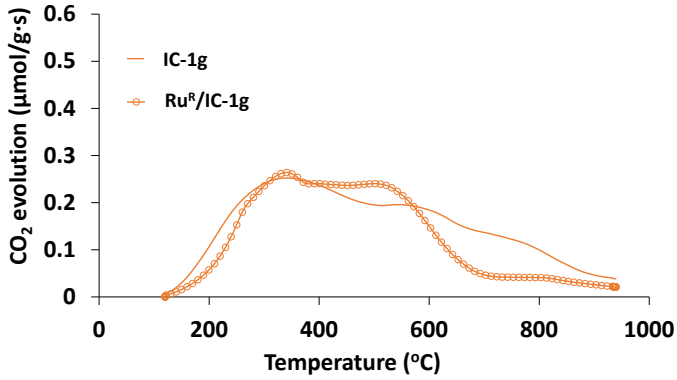

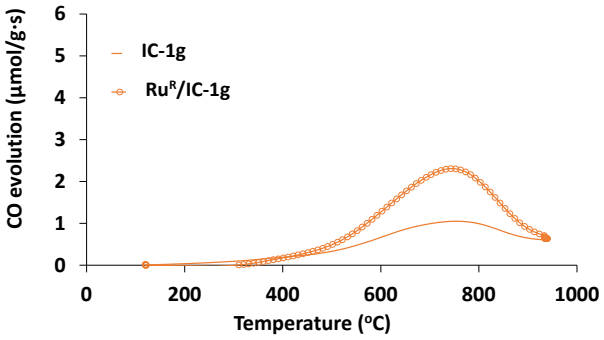

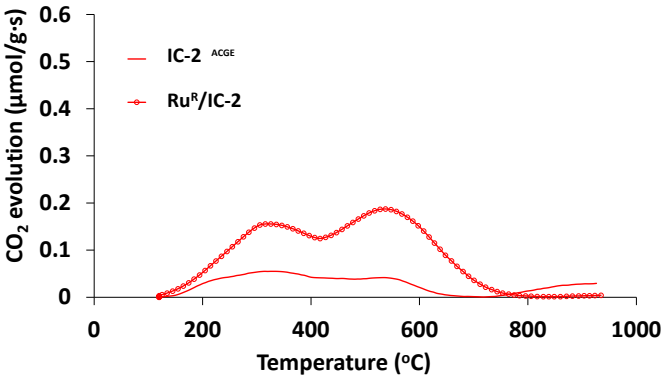

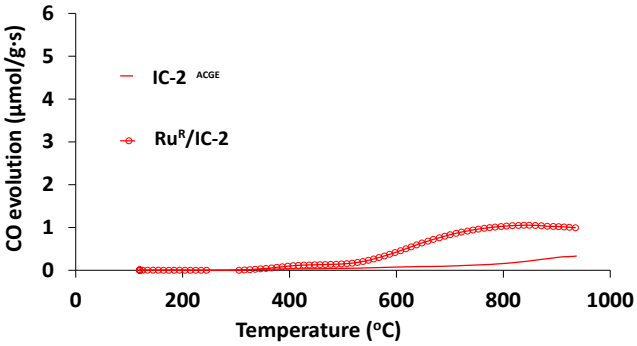

Table S4. Decomposition temperature of OFG on carbon materials in TPD experiments [2,3].

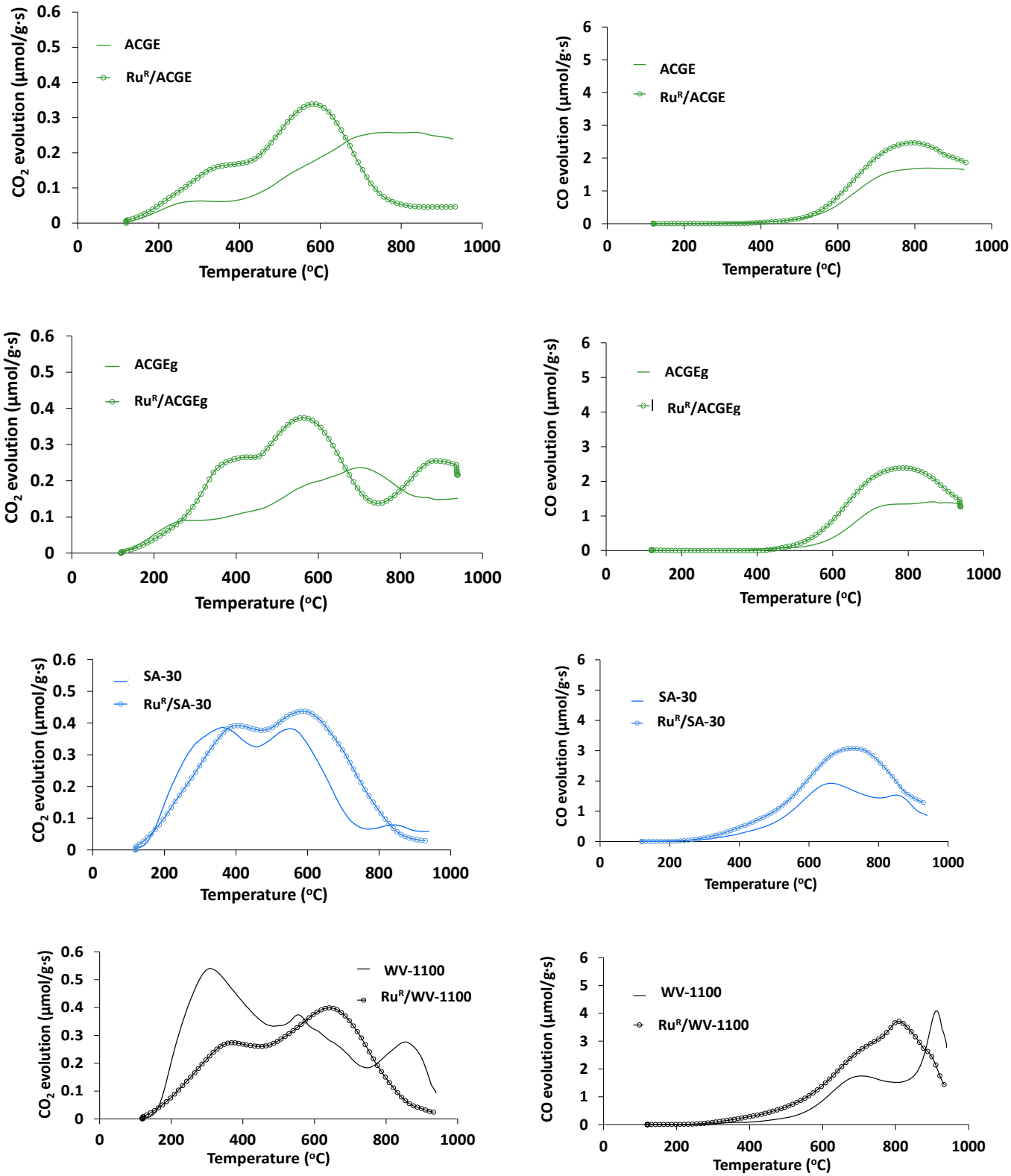

Fig. S5. TPD spectra of carbon supports and reduced catalysts: CO_2 and CO evolution (be aware of the different scale in y-axis).

Table S5. Amount of CO_2 and CO evolved in TPD experiments, and the corresponding total oxygen of carbon supports and the corresponding as prepared and reduced catalysts.

Sample	CO_2 (µmol/g)	CO (µmol/g)	O_{total} (wt. %)
IC-1	258	928	2.3
Ru^R/IC-1	239	2135	4.2
IC-1g	374	1172	3.1

Ru^R/IC-1g	313	2071	4.3
IC-2	68	208	0.6
Ru^R/IC-2	209	1026	2.3
ACGE	351	1559	3.6
Ru^R/ACGE	361	2169	4.6
ACGEg	342	1267	3.1
Ru^R/ACGEg	509	2123	5.0
SA-30	539	2065	5.0
Ru^R/SA-30	615	3168	7.0
WV-1100	735	2202	5.9
Ru^R/WV-1100	526	3151	6.7

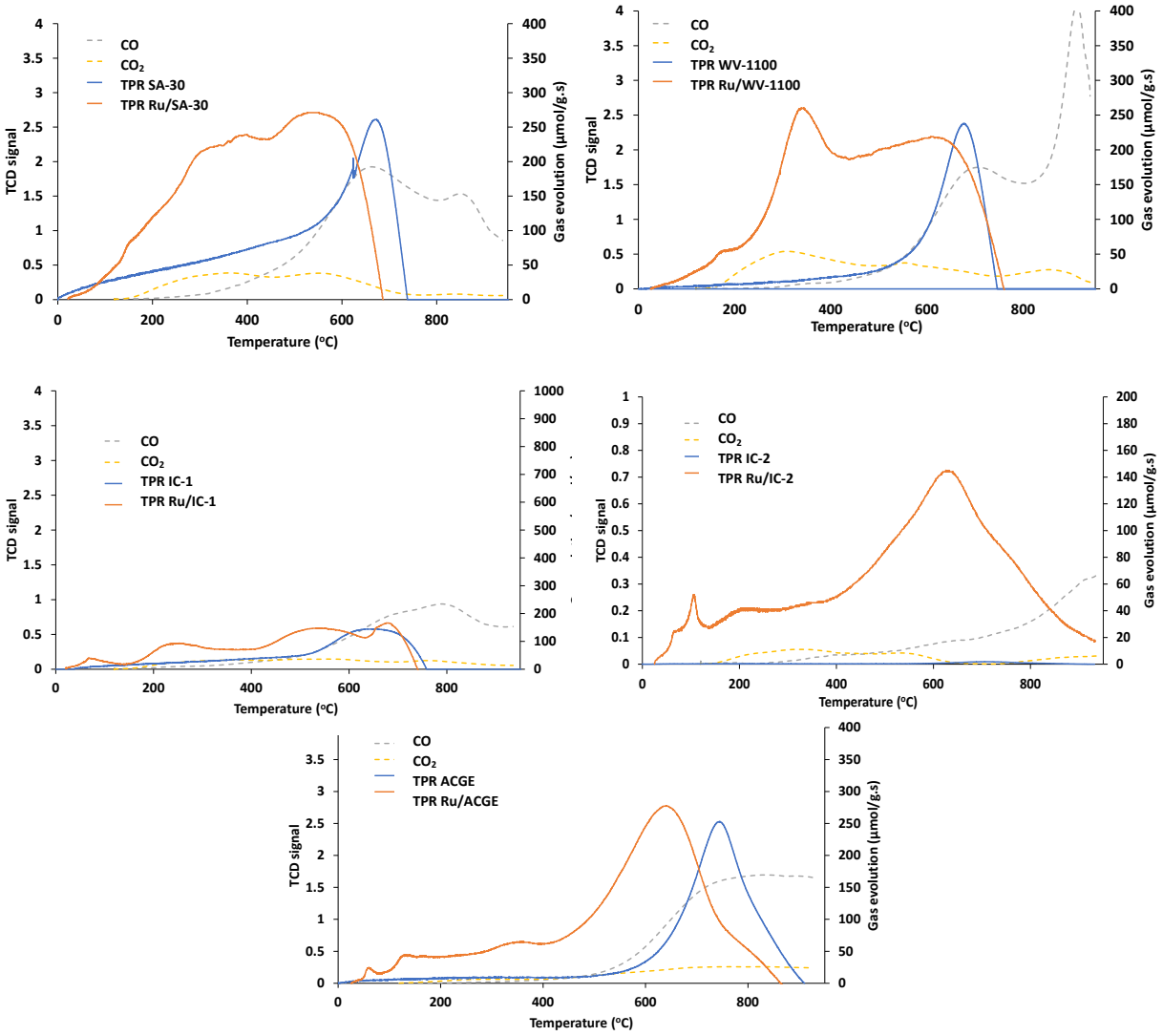

Fig. S6 TPD (right axis) and TPR (left axis) signals of Ru/C catalysts.

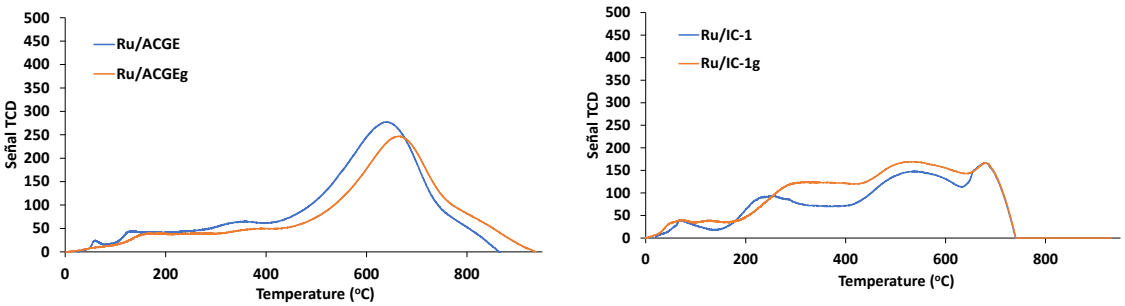

Fig. S7 Comparison of H2-TPR's profiles for the spherical catalysts and the grounded counterparts.

Table S6. O wt.% corresponding to different oxygen species determined by XPS.

		O wt.%		
	Species	**O 1***	**O 2***	**O 3***
	BE (eV)	531	533	534
Catalysts	Ru/IC-1	3.5	3.7	1.6
	Ru^R/IC-1	1.7	3.1	0.7
	Ru/IC-2	2.3	2.7	1.0
	Ru^R/IC-2	1.8	2.6	0.6
	Ru/ACGE	2.9	3.3	1.7
	Ru^R/ACGE	2.6	3.4	1.9
	Ru/SA-30	5.1	5.0	2.8
	Ru^R/SA-30	3.0	3.5	1.2
	Ru/WV-1100	4.4	6.0	2.2
	Ru^R/WV-1100	3.9	4.1	1.4

*O1- carbonyl and anhydride groups (B.E.≈531 eV), O2 -phenol groups (B.E≈533 eV) and O3-carboxylic groups (B.E.≈534 eV)

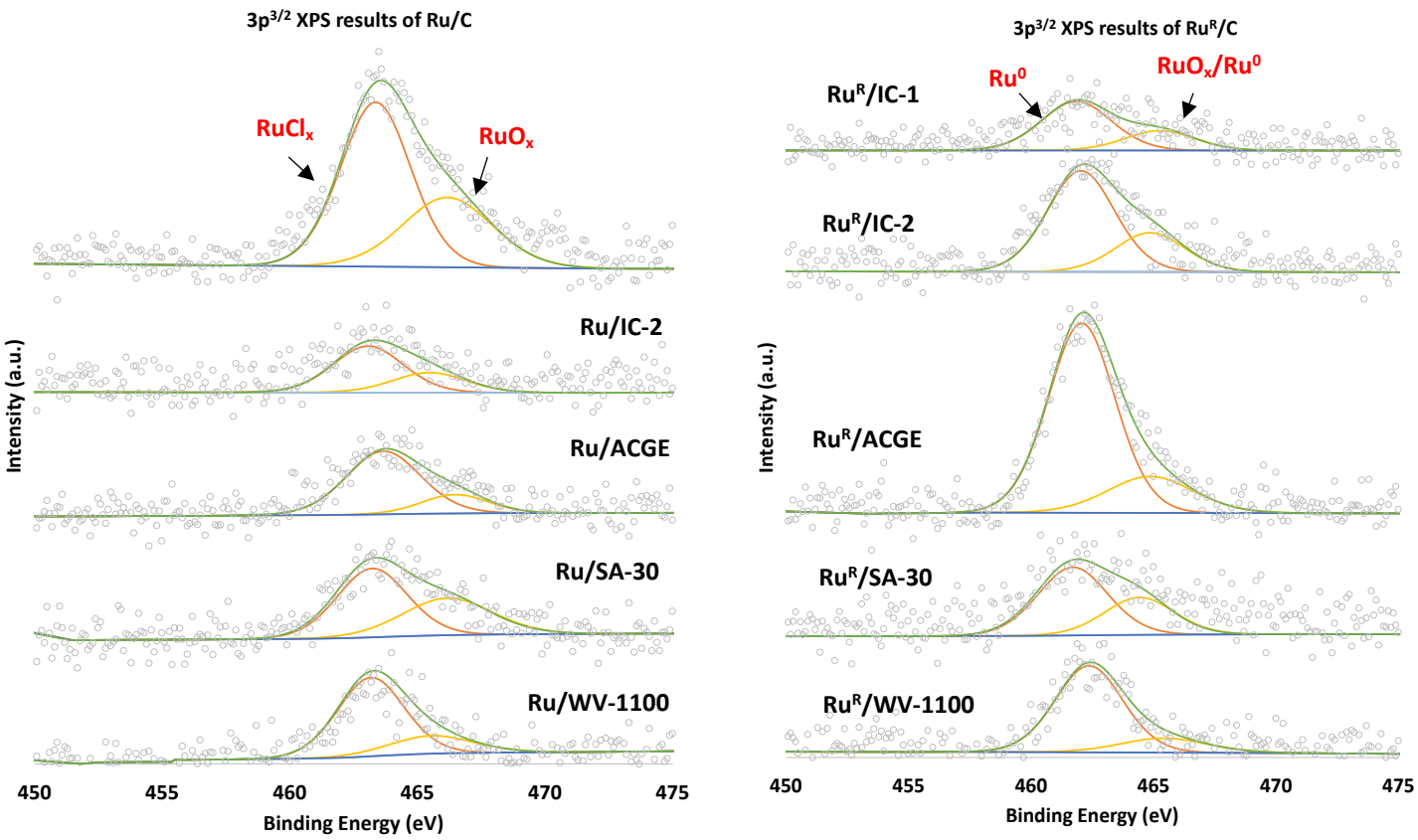

Fig. S8 Ru $3p_{3/2}$ XPS results of the Ru/C catalysts (as prepared on the left and reduced on the right).

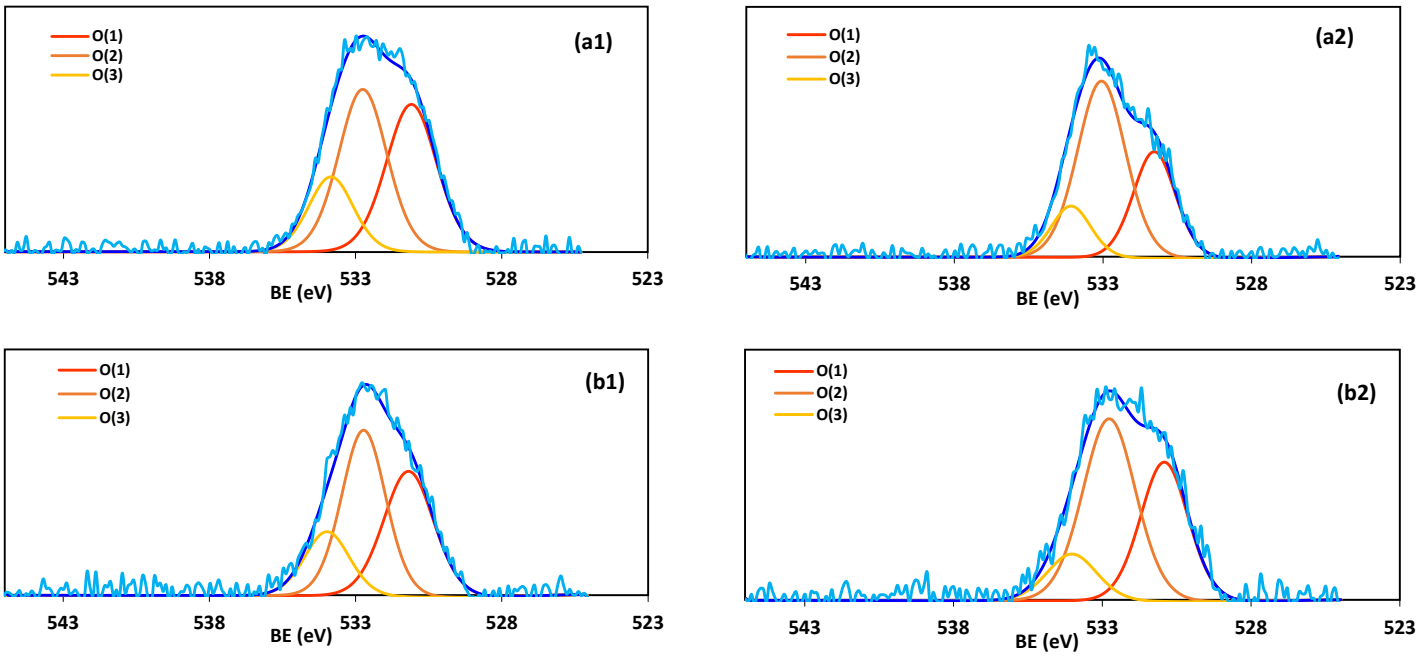

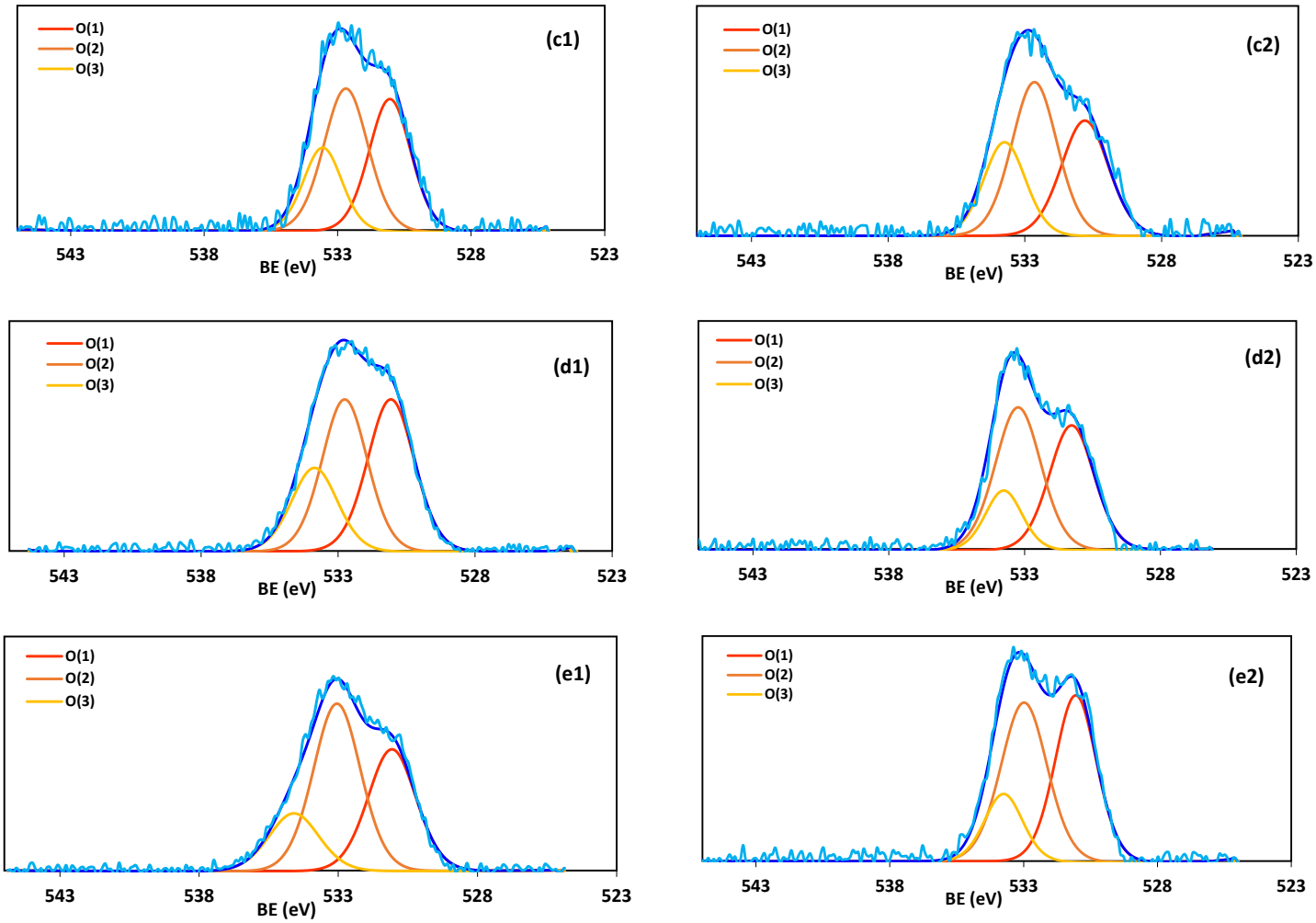

Fig. S9 O1s XPS data of the Ru/C (1) and Ru^{R}/C (2) catalysts where C is: a) IC-1 , b) IC-2 c) ACGE, d) SA-30 and e) WV-1100. Identified of oxygen species is as follows: O1- carbonyl and anhydride groups (B.E.≈531 eV), O2 -phenol groups (B.E≈533 eV) and O3-carboxylic groups (B.E.≈534 eV) [4–6].

Ru^{R}/SA-30 (previously reduced)

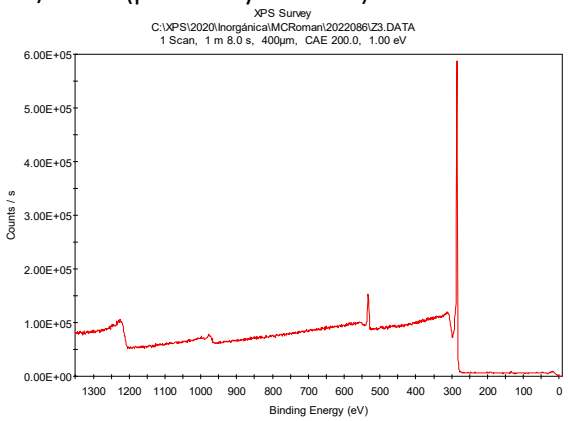

Ru/SA-30 (fresh)

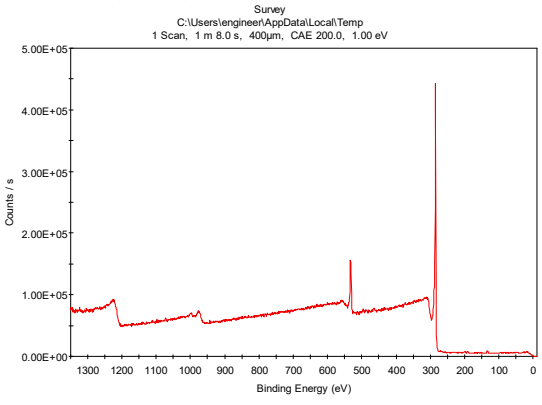

Ru^{R}/WV-1100 (previously reduced)

Ru/WV-1100 (fresh)

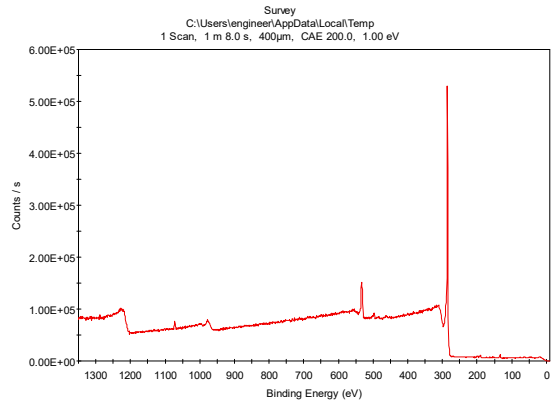

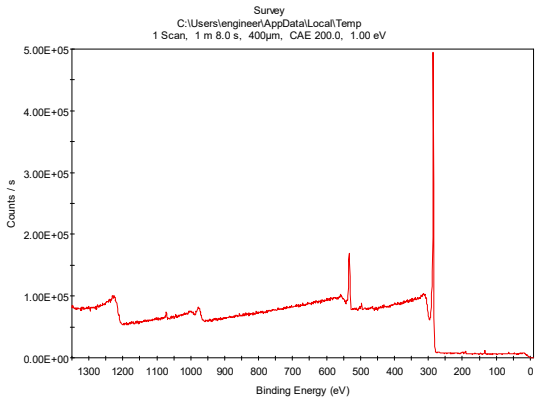

Ru^{R}/IC-1 (previously reduced)

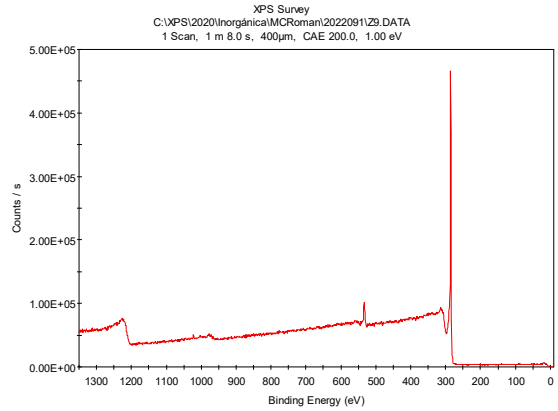

Ru/IC-1 (fresh)

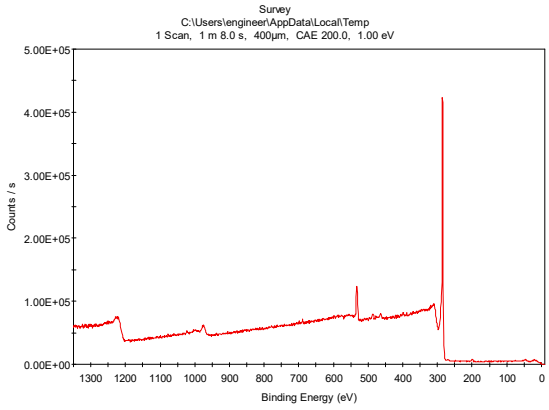

Ru^{R}/IC-2 (previously reduced)

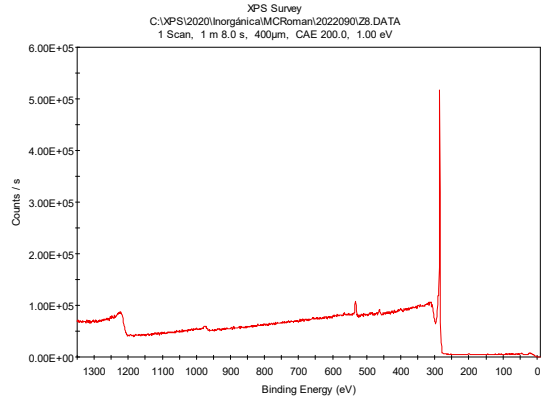

Ru/IC-2 (fresh)

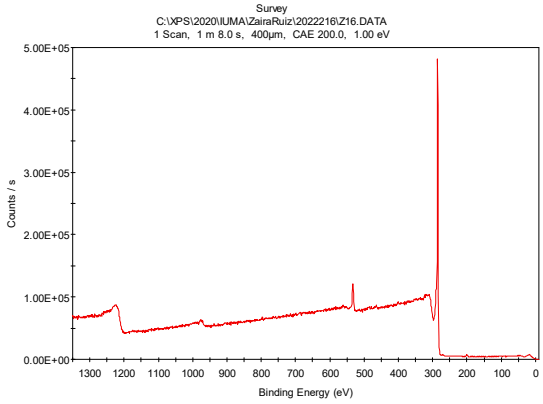

Ru^R/ACGE (previously reduced)

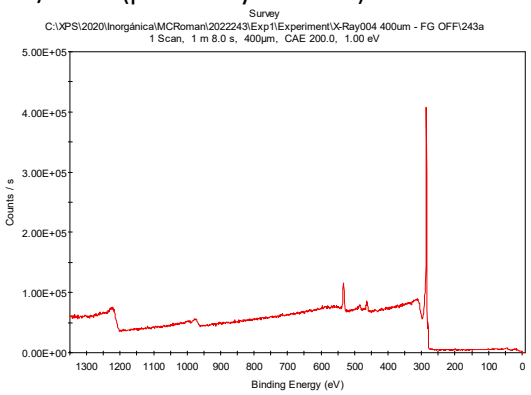

Ru/ACGE (fresh)

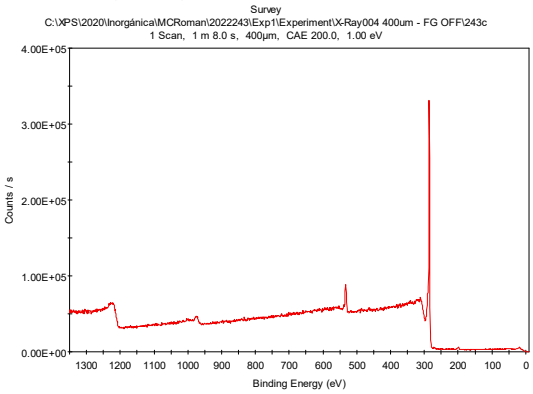

Fig. S10 Survey XPS data

Table S7. Atomic % of the elements determined by XPS in the Ru/C catalysts

	At.%					
Catalyst	Ru	C	O	Cl	P	total
Ru/IC-1	0.82	91.32	7.24	0.62	-	100
Ru^R/IC-1	0.24	95.18	4.31	0.2	-	100
Ru/IC-2	0.24	94.66	4.70	0.4	-	100
Ru^R/IC-2	0.46	95.34	3.92	0.27	-	100
Ru/ACGE	0.39	92.73	6.3	0.58	-	100
Ru^R/ACGE	0.91	92.4	6.49	0.20	-	100
Ru/SA-30	0.32	88.41	10.32	0.27	0.66	99.98
Ru^R/ SA-30	0.27	93.14	6.02	0.05	0.51	99.99
Ru/WV-1100	0.25	88.56	10.12	0.23	0.83	99.99
Ru^R/WV-1100	0.29	90.88	7.55	0.29	0.98	99.99
Ru/IC-1 used	2.38	78.3	19.23	0.1	0	100
Ru/SA-30 used	0.24	86.29	9.96	0.1	0.44	100

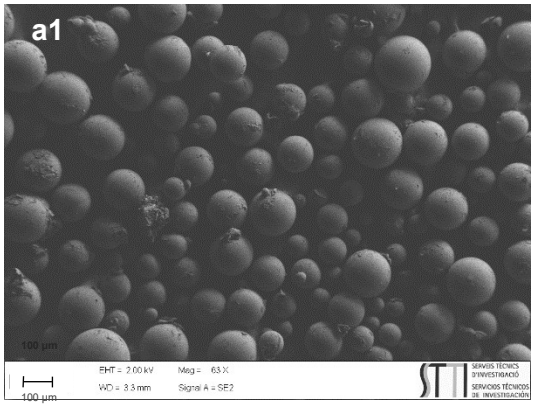

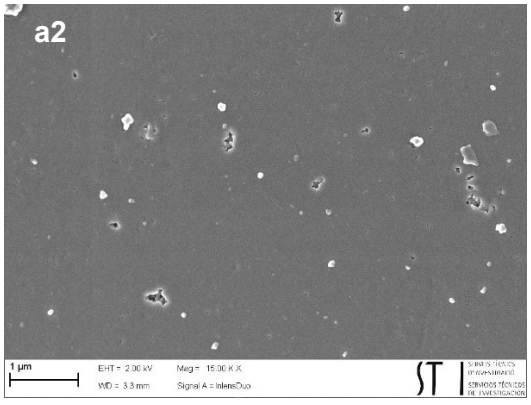

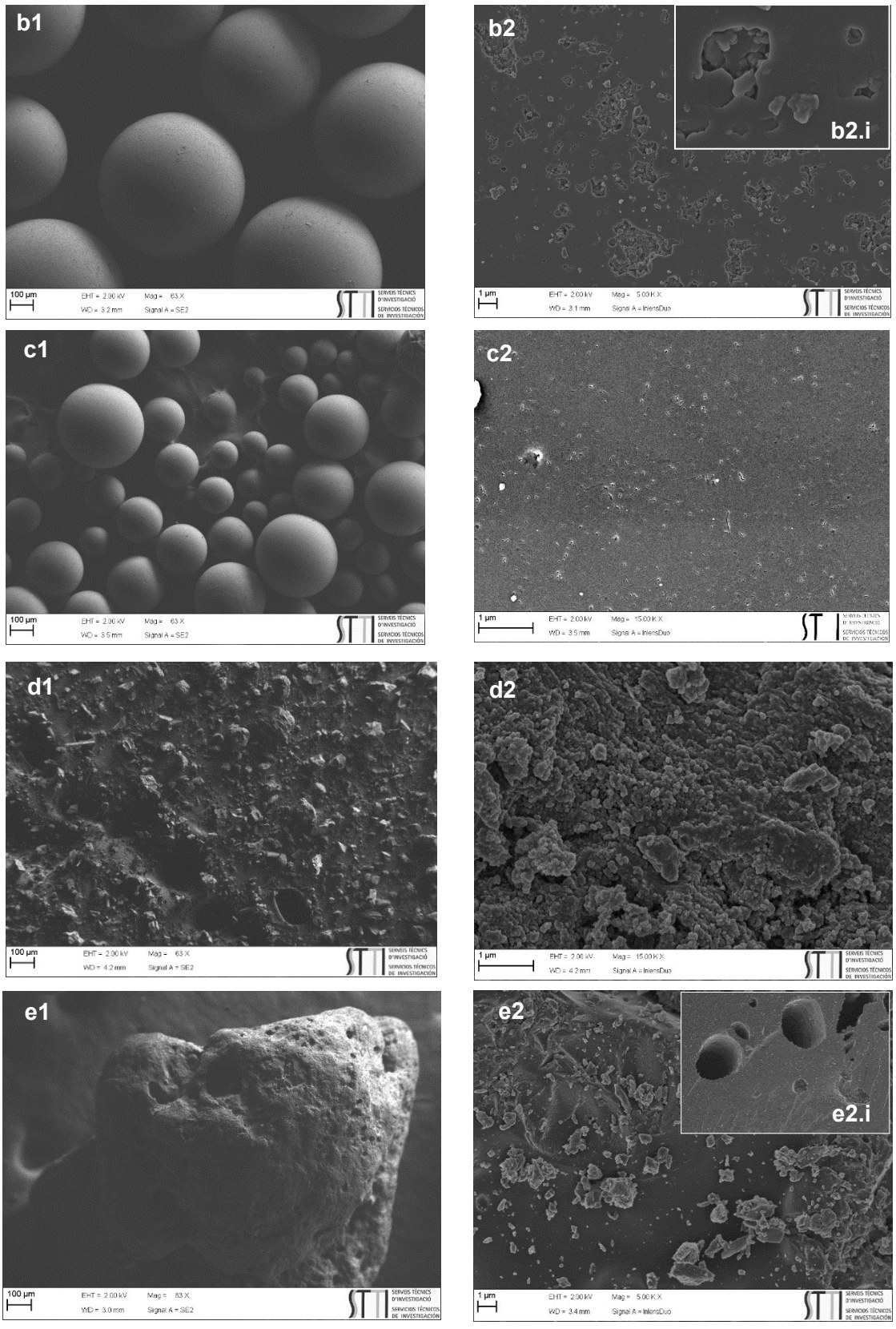

Fig. S11 FESEM images of carbon materials: IC-1 (a1 and a2), IC-2 (b1, b2 and b2.i), ACGE (c1 and c2), SA-30 (d1 and d2) and WV-1100 (e1, e2 and e2.i).

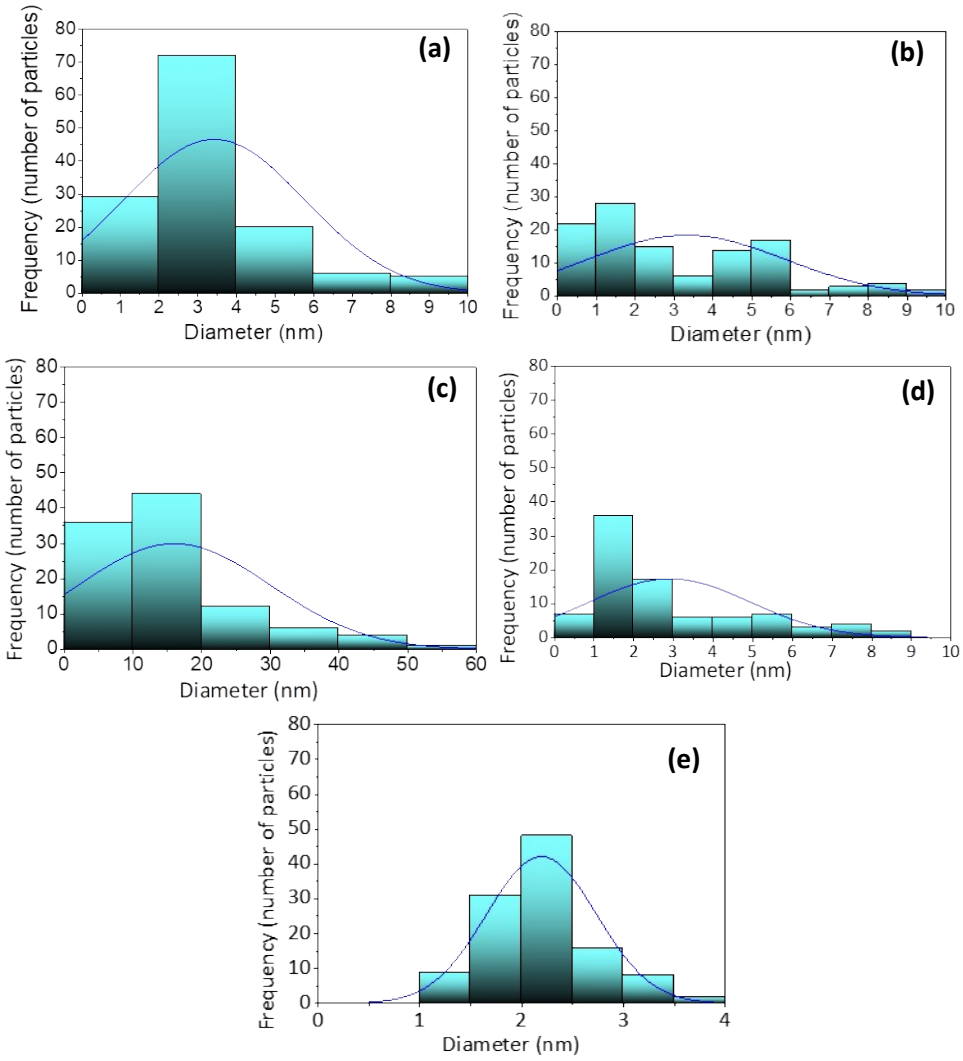

Fig. S12 Particle size distribution for: (a) Ru^R/IC-1, (b) Ru^R/IC-2, (c) Ru^R/ACGE, (d) Ru^R/SA-30 and (e) Ru^R/WV-1100 (be aware of the different scale in x-axis of the different figures).

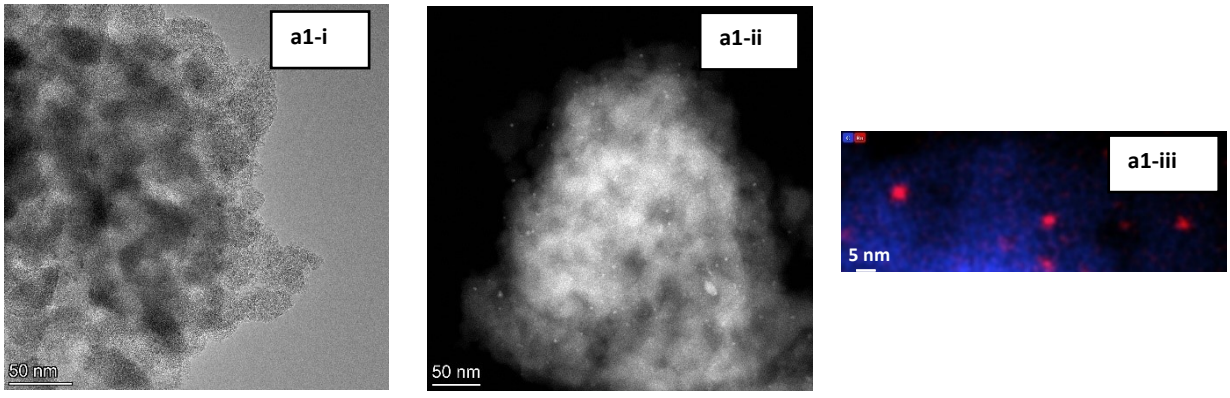

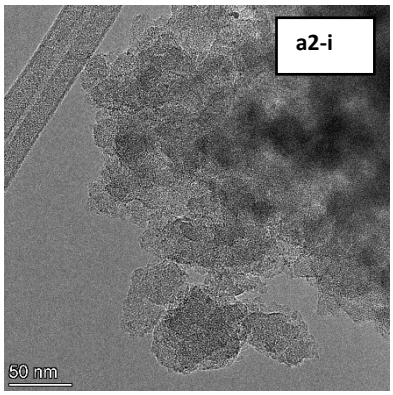
a2-i
50 nm

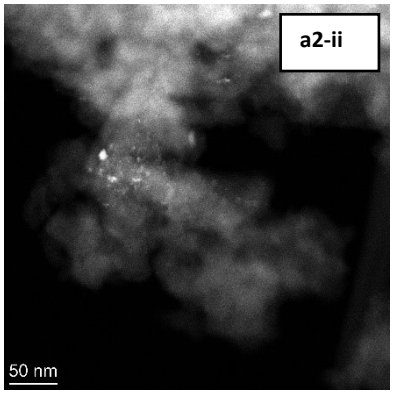
a2-ii
50 nm

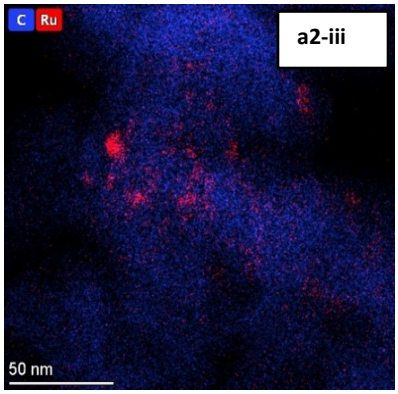
C
Ru
a2-iii
50 nm

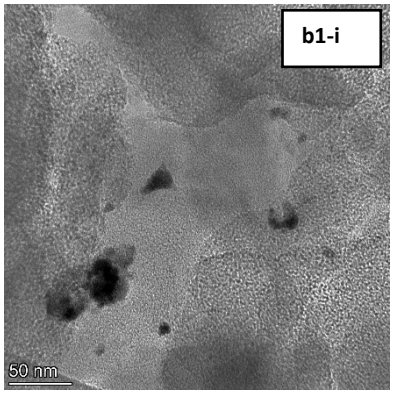
b1-i
50 nm

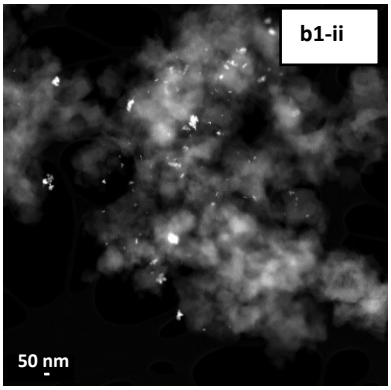
b1-ii
50 nm

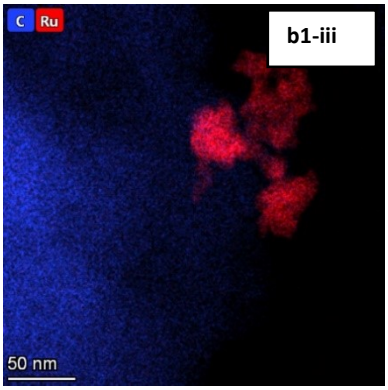
C
Ru
b1-iii
50 nm

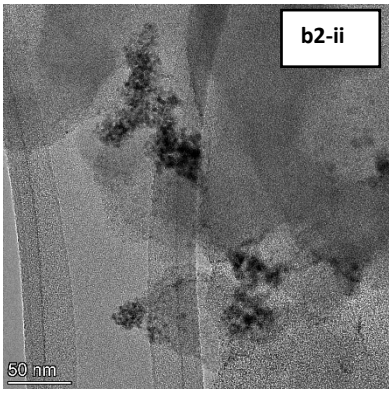
b2-ii
50 nm

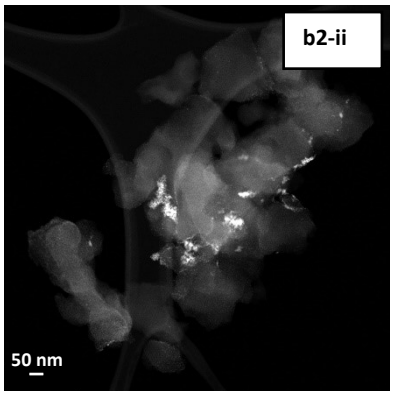
b2-ii
50 nm

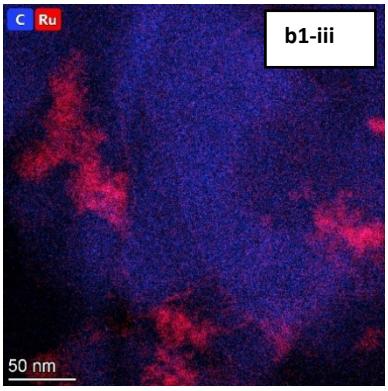
C
Ru
b1-iii
50 nm

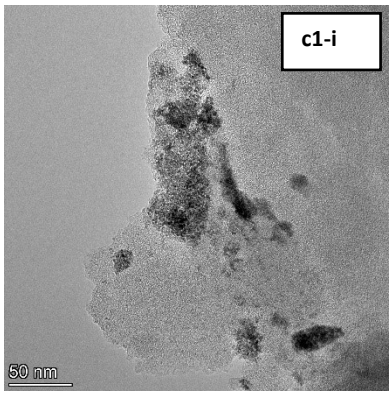
c1-i
50 nm

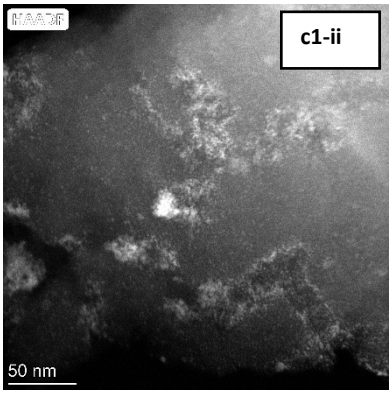
HAADF
c1-ii
50 nm

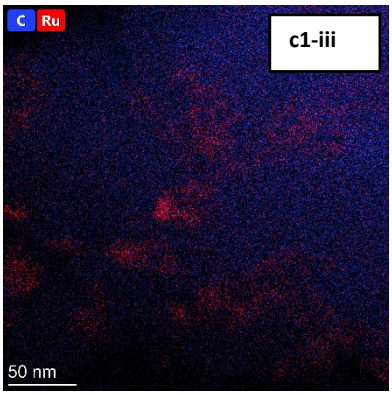
C
Ru
c1-iii
50 nm

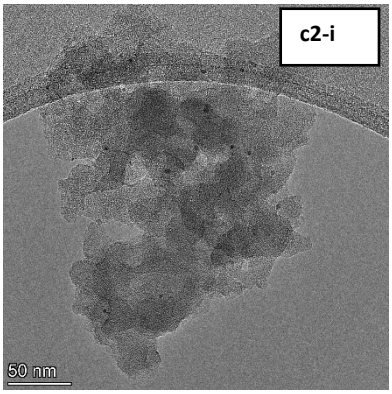
c2-i
50 nm

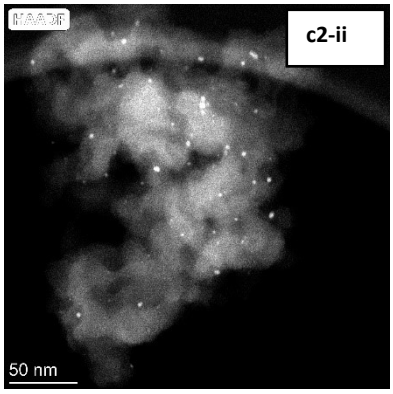
HAADF
c2-ii
50 nm

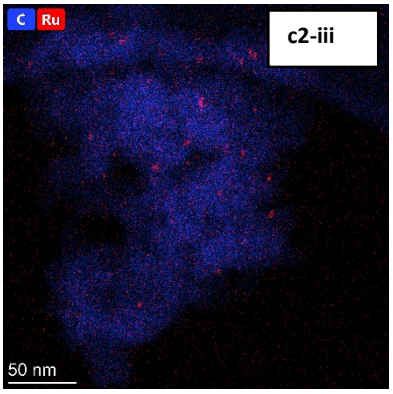
C
Ru
c2-iii
50 nm

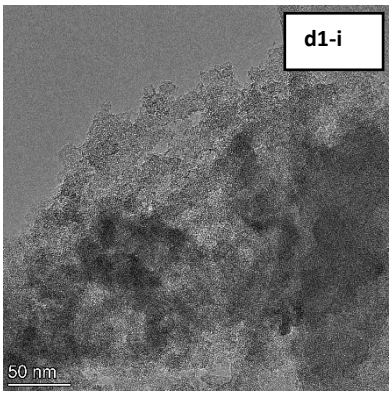
d1-i
50 nm

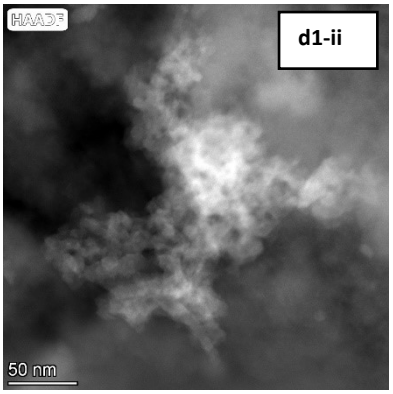
HAADF
d1-ii
50 nm

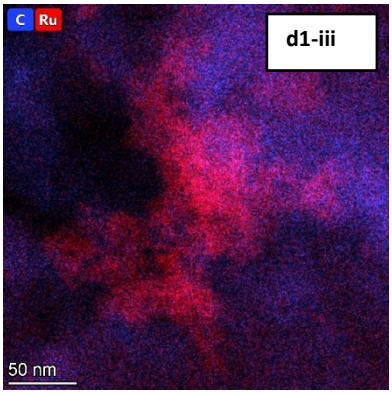
C
Ru
d1-iii
50 nm

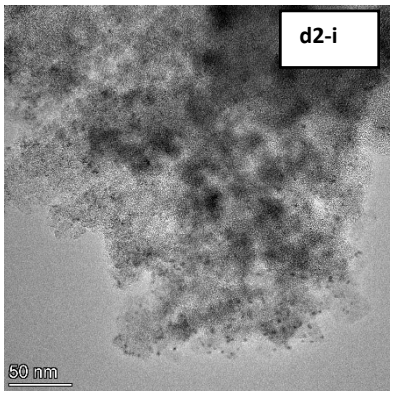
d2-i
50 nm

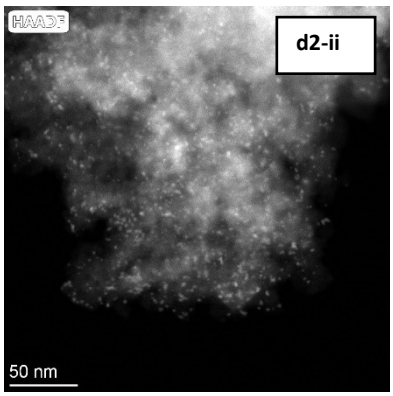
HAADF
d2-ii
50 nm

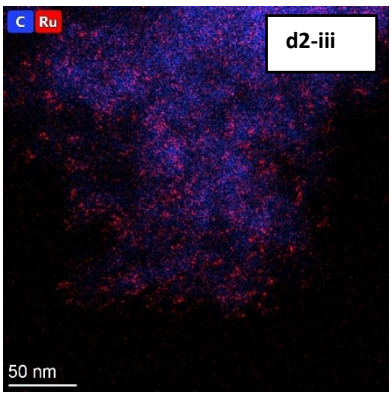
C
Ru
d2-iii
50 nm

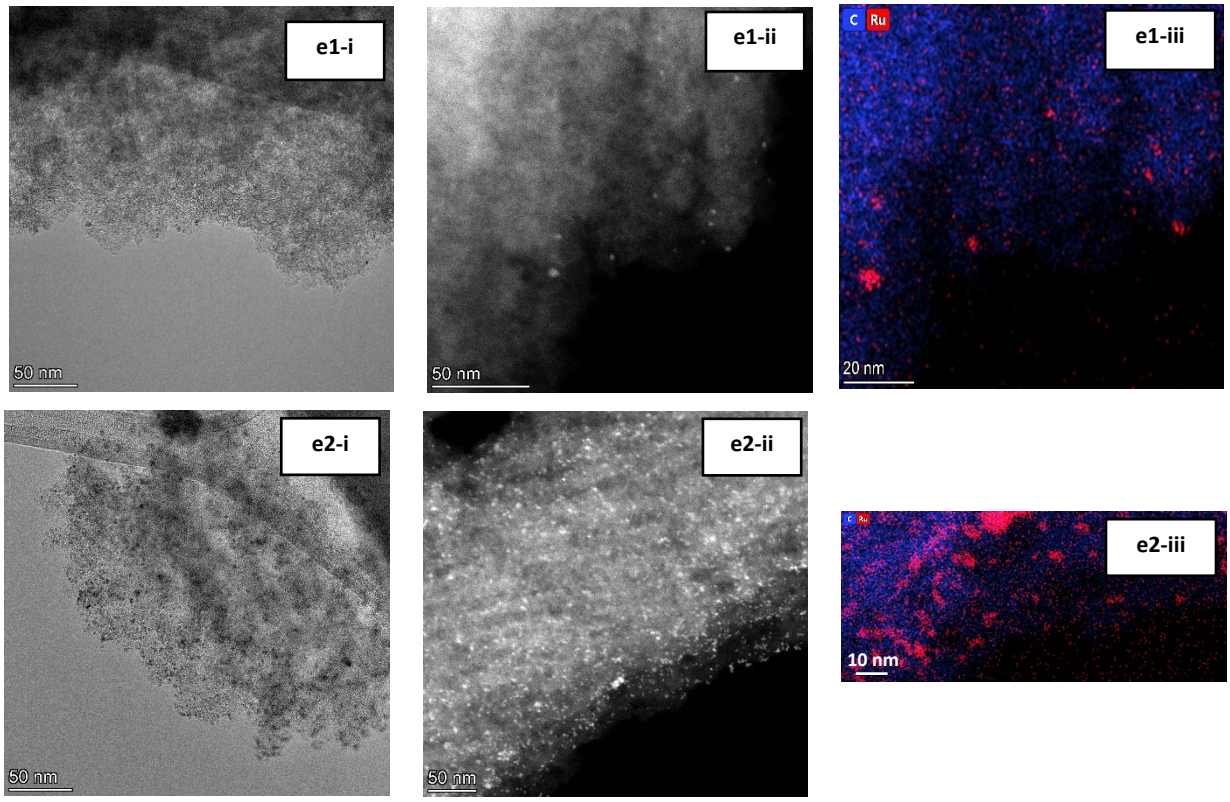

Fig. S13 TEM images of spent catalysts that have been either used as prepared (images a1-e1) and previous reduced (images a2-e2) (reaction conditions: 70ºC, 15 bar H_2, 1 h). Each letter refers to the catalyst prepared with each support: a for IC-1, b for IC-2, c for ACGE, d for SA-30 and e for WV-1100. The first column corresponds to TEM images (i), the second corresponds to STEM HAAF (ii) and the third one to EDX images (iii).

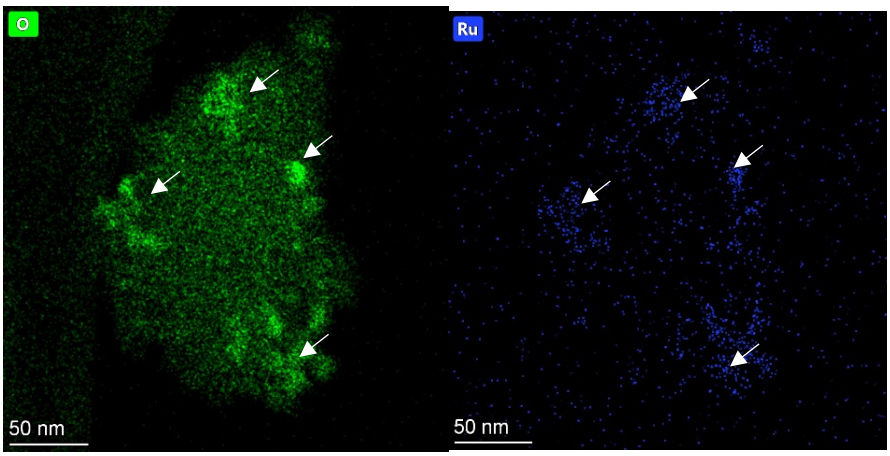

Fig. S14. O and Ru mapping of the Ru/WV catalyst

References:

1 A. P. Terzyk, P. A. Gauden and P. Kowalczyk, *Carbon*, 2002, **40**, 2879–2886.

2 J. L. Figueiredo, M. F. R. Pereira, M. M. A. Freitas and J. J. M. Órfão, *Carbon*, 1999, **37**, 1379–1389.

3 G. S. Szymański, Z. Karpiński, S. Biniak and A. Świątkowski, *Carbon*, 2002, **40**, 2627–2639.

4 F.-Z. Azar, M. A. Lillo-Ródenas and M. C. Román-Martínez, *SN Appl. Sci.*, 2019, **1**, 1739.

5 I. Velo-Gala, J. J. López-Peñalver, M. Sánchez-Polo and J. Rivera-Utrilla, *Carbon,* 2014, **67**, 236–249.

6 T. I. T. Okpalugo, P. Papakonstantinou, H. Murphy, J. McLaughlin and N. M. D. Brown, *Carbon*, 2005, **43**, 153-161.